Inorg. Chem. **2004**, *43*, 6414–6420

Vanadium 7,7,8,8-Tetracyano-*p*-quinodimethane (V[TCNQ]$_2$)-Based Magnets

Elaine B. Vickers, Trent D. Selby, Matthew S. Thorum, Michelle L. Taliaferro, and Joel S. Miller*

Department of Chemistry, University of Utah, 315 S. 1400 East, Room 2124, Salt Lake City, Utah 84112-0850

Received April 5, 2004

A new family of molecule-based magnets of general formula V[TCNQR$_2$]$_2$·*z*CH$_2$Cl$_2$ has been synthesized and characterized (TCNQ = 7,7,8,8-tetracyano-*p*-quinodimethane; R = H, Br, Me, Et, *i*-Pr, OMe, OEt, and OPh). In addition, solid solutions of V[TCNQ]$_x$[TCNQ(OEt)$_2$]$_{2-x}$·*z*CH$_2$Cl$_2$ composition have been prepared. Except R = Br, magnetic ordering was observed for all materials, with T_c values between 7.5 K (R = Me) and 106 K (R = OEt), with R = H at 52 K. The substitution of electron-donating OMe and OEt groups for H in TCNQ increased T_c, whereas the substitution of less electron-donating alkyl groups (with respect to alkoxy groups) decreased T_c. The results of MO calculations indicate that neither the spin nor charge densities of the disubstituted TCNQs are sufficiently different to explain the wide range of critical temperatures. Although the structures of the amorphous materials are not known, it is proposed that the oxygen atom of the [TCNQR$_2$]$^{\bullet-}$ acceptor (R = OMe and OEt) and the V(II) interact to form a seven-membered ring. This interaction could stabilize the structure and enhance the magnetic coupling, leading to an increased T_c. The magnetic properties of V[TCNQ]$_x$[TCNQ(OEt)$_2$]$_{2-x}$·*z*CH$_2$Cl$_2$ deviated from the expected linear relationship with respect to *x*, exhibiting magnetic behavior more characteristic of a step function in a plot of T_c versus *x*.

Introduction

Magnetically ordered molecule-based materials constitute a growing area of contemporary chemistry.[1,2] [Fe(C$_5$Me$_5$)$_2$]$^{\bullet+}$-[TCNE]$^{\bullet-}$ (TCNE = tetracyanoethylene) was the first organic-containing molecule-based magnet characterized, and it orders as a ferromagnet below a critical temperature, T_c, of 4.8 K.[3] Further work led to the discovery of V[TCNE]$_y$·*z*CH$_2$Cl$_2$, the first room-temperature organic magnet ($T_c \sim$ 400 K), initially from the reaction of TCNE and V^0(C$_6$H$_6$)$_2$[4] and later from the reaction of TCNE and V^0(CO)$_6$.[5] Utilization of the latter volatile precursors led to the development of a chemical vapor deposition (CVD) route to solvent-free thin films of the V[TCNE]$_y$ magnet that also exhibited enhanced air stability.[6]

V[TCNE]$_y$ is an amorphous, disordered material with a small coercive field, H_{cr}, < 1 Oe at room temperature and

* To whom correspondence should be addressed. E-mail: jsmiller@chem.utah.edu.

(1) (a) In *Molecular Crystals and Liquid Crystals*, Proceedings of the conference on Ferromagnetic and High Spin Molecular Based Materials; Miller, J. S., Dougherty, D., Eds.; 1989; Vol. 176. (b) In *NATO ARW Molecular Magnetic Materials*, Proceedings of the conference on Molecular Magnetic Materials; Kahn, O., Gatteschi, D., Miller, J. S., Palacio, F., Eds.; 1991; Vol. E198. (c) In *Molecular Crystals and Liquid Crystals*, Proceedings of the conference on the Chemistry and Physics of Molecular Based Magnetic Materials; Iwamura, H., Miller, J. S., Eds.; 1993; Vol. 232/233. (d) In *Molecular Crystals and Liquid Crystals*, Proceedings of the conference on Molecule-based Magnets; Miller, J. S., Epstein, A. J., Eds.; 1995; Vol. 271−274. (e) In *Molecular Crystals and Liquid Crystals*, Proceedings of the conference on Molecular-Based Magnets; Itoh, K., Miller, J. S., Takui, T., Eds.; 1997; Vol. 305/306. (f) Turnbull, M. M.; Sugimoto, T.; Thompson, L. K., Eds. *ACS Symp. Ser.* **1996**, *644*.

(2) Reviews: (a) Miller, J. S.; Epstein, A. J. *Chem. Commun.* **1998**, 1319. (b) Ovcharenko, V. I.; Sagdeev, R. Z. *Russ. Chem. Rev.* **1968**, *68*, 345. (c) Plass, W. *Chem. Ztg.* **1998**, *32*, 323. (d) Miller, J. S.; Epstein, A. J. *Chem. Eng. News* **1995**, *73* (40), 30. (e) Miller, J. S.; Epstein, A. J. *Angew. Chem., Int. Ed. Engl.* **1994**, *33*, 385. (f) Kinoshita, M. *Jpn. J. Appl. Phys.* **1994**, *33*, 5718. (g) Miller, J. S.; Epstein, A. J. *Adv. Chem. Ser.* **1995**, *245*, 161. (h) Caneschi, A.; Gatteschi, D. *Prog. Inorg. Chem.* **1991**, *37*, 331. (i) Buchachenko, A. L. *Russ. Chem. Rev.* **1990**, *59*, 307.

(3) (a) Miller, J. S.; Calabrese, J. C.; Epstein, A. J.; Bigelow, R. W.; Zhang, J. H.; Reiff, W. M. *J. Chem. Soc., Chem. Commun.* **1986**, 1026. (b) Miller, J. S.; Calabrese, J. C.; Rommelmann, H.; Chittipeddi, S.; Zhang, J. H.; Reiff, W. M.; Epstein, A. J. *J. Am. Chem. Soc.* **1987**, *109*, 769.

(4) (a) Manriquez, J. M.; Yee, G. T.; McLean, R. S.; Epstein, A. J.; Miller, J. S. *Science* **1991**, *252*, 1415. (b) Epstein, A. J.; Miller, J. S. In the Proceedings of Nobel Symposium NS-81 *Conjugated Polymers and Related Materials: The Interconnection of Chemical and Electronic Structure*; Oxford University Press: Oxford, 1993, p 475; *La Chim. La Ind.* **1993**, *75*, 185, 257. (c) Miller, J. S.; Yee, G. T.; Manriquez, J. M.; Epstein, A. J. In the Proceedings of Nobel Symposium NS-81 *Conjugated Polymers and Related Materials: The Interconnection of Chemical and Electronic Structure*; Oxford University Press: Oxford, 1993, p 461; *La Chim. La Ind.* **1992**, *74*, 845.

(5) Zhang, J.; Zhou, P.; Brinckerhoff, W. B.; Epstein, A. J.; Vazquez, C.; McLean, R. S.; Miller, J. S. *ACS Symp. Ser.* **1996**, *644*, 311−318.

10.1021/ic049552z CCC: $27.50
Published on Web 09/04/2004

7.4 Oe at 5 K.[7] Furthermore, it is a magnetic semiconductor with a room-temperature conductivity of $\sim 10^{-4}$ S/cm, and recent magnetotransport studies indicate that electrons in valence and conducting bands are spin polarized, suggesting "spintronic" applications.[8]

In contrast, the reactions of $Fe(CO)_5$ with TCNE and TCNQ (TCNQ = 7,7,8,8-tetracyano-*p*-quinodimethane, **1**) form $Fe[TCNE]_2 \cdot zCH_2Cl_2$ and $Fe[TCNQ]_2 \cdot zCH_2Cl_2$ that magnetically order at 100 and 35 K, respectively.[9] To date, the reaction of TCNQ and $V^0(CO)_6$ has not been reported to form a magnetically ordered material. Other $M[TCNQ]_2$ materials for M ≠ V, however, have previously been reported[10] as solvates with methanol or water,[10c] products of electrochemical synthesis,[10d] and products from $Fe(CO)_5$[9] and $[M(NCMe)_6][BF_4]_2$[10f] starting materials. Herein, the reactions of $V^0(CO)_6$ with TCNQ and several 2,5-disubstituted TCNQs (**2**) are explored, and several new magnetically ordered materials are reported.

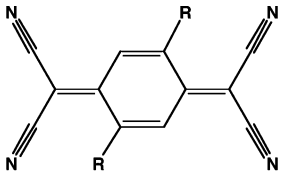

1: R = H; **2a**: R = Br; **b**: R = Me; **c**: R = Et; **d**: R = *i*-Pr; **e**: R = OMe; **f**: R = OEt; **g**: R = OPh

Experimental Section

Due to the extreme air and water sensitivity of the materials studied, all manipulations and reactions were performed in a Vacuum Atmospheres DriLab glovebox (<1 ppm O_2 and <1 ppm H_2O). CH_2Cl_2 was dried over two columns of activated alumina.[11] $[N(n\text{-}Bu)_4]I$ was obtained from Aldrich. $V(CO)_6$ was prepared from $[NEt_4][V(CO)_6]$ via a literature preparation[12] and was sublimed at 25 °C and 50 mTorr. TCNQ and the substituted TCNQs (**2**)[13] were gifts from DuPont (**2a**−**d**, **2g**) and were purified prior to use. Compounds **2e**,**f** were kindly provided by Prof. G. Saito and H. Yamochi (Kyoto University). $[V^{II}(NCMe)_6][BPh_4]_2$ was prepared via a literature procedure.[14] The compositions are reproducible except for small variations in the amount of solvent, and small differences in T_c are attributed to the extreme air sensitivity of the materials.

$[N(n\text{-}Bu)_4][TCNQ]$. $[N(n\text{-}Bu)_4]I$ (5.96 mmol) was dissolved in 8 mL of hot acetonitrile and added dropwise to a stirred solution of TCNQ (4.00 mmol dissolved in 90 mL) in hot acetonitrile, immediately causing the solution to turn dark green. The solution was then heated until the volume had been reduced to 10 mL, after which it was allowed to cool to room temperature and put in the freezer overnight. Dark blue, crystalline product was then filtered and dried for 3 h under vacuum (yield ∼ 95%).

$V[TCNQ]_2 \cdot zCH_2Cl_2$. This material was prepared from $V(CO)_6$. In a typical preparation, $V(CO)_6$ (0.137 mmol) was dissolved in 5 mL of CH_2Cl_2 and added dropwise to a stirred solution of TCNQ (0.274 mmol) in 30 mL of CH_2Cl_2. The solution quickly turned dark with the evolution of CO and was allowed to react 15 min without stirring, but with venting. The dark, amorphous product was filtered, washed with CH_2Cl_2, and dried (yield ∼ 85%). The observed elemental analysis (calcd[15]) for $V[TCNQ]_2 \cdot zCH_2Cl_2$ follows: $z = 0.84$, $VC_{24.84}H_{9.68}N_8Cl_{1.68}$, %C = 55.78 (56.23), %H = 2.15 (1.84), %N = 21.57 (21.12).

The synthesis of $V[TCNQ]_2 \cdot zCH_2Cl_2$ was also attempted via the following three synthetic pathways in CH_2Cl_2 (eqs 1−3):

$$[V(NCMe)_6][BPh_4]_2 + 2[N(n\text{-}Bu)_4][TCNQ] \rightarrow V[TCNQ]_2 + 2[N(n\text{-}Bu)_4]^+ + 2[BPh_4]^- \quad (1)$$

$$[NEt_4][V(CO)_6] + 3TCNQ \rightarrow V[TCNQ]_2 + 6CO + [NEt_4]^+ + [TCNQ]^- \quad (2)$$

$$[NEt_4][V(CO)_6] + 5[N(n\text{-}Bu)_4][TCNQ] \rightarrow V[TCNQ]_2 + 6CO + [NEt_4]^+ + 5[N(n\text{-}Bu)_4]^+ + 3[TCNQ]^{2-} \quad (3)$$

Unfortunately, infrared and elemental analysis data indicate that the products of these reactions contain significant amounts of impurities (MeCN, $[BPh_4]^-$, $[N(n\text{-}Bu)_4]^+$, $[NEt_4]^+$, and/or $[TCNQ]^{2-}$). The products of these three reactions do not magnetically order. $\nu_{C\equiv N}$ IR (KBr): 2197s, 2113s cm^{-1} (eq 1); 2187s, 2098s, 2030sh cm^{-1} (eq 2); and 2187s, 2103s, 2033sh cm^{-1} (eq 3). The products of eqs 1−3 show their strongest $\nu_{C\equiv N}$ IR absorption at higher energy than $V[TCNQ]_2 \cdot zCH_2Cl_2$ from $V(CO)_6$ (2088 cm^{-1}). In addition, the low energy $\nu_{C\equiv N}$ shoulder observed in $V[TCNQ]_2 \cdot zCH_2Cl_2$ from $V(CO)_6$ (2024 cm^{-1}) is present in the products of eqs 2 and 3, but not in the product of eq 1.

$V[TCNQR_2]_2 \cdot zCH_2Cl_2$. Substitution of TCNQ with 2,5-disubstituted TCNQs in the above procedure from $V(CO)_6$ led to formation of materials possessing vanadium and the 2,5-disubstituted TCNQ (**2**). The observed elemental analysis (calcd) for $V[TCNQBr_2]_2 \cdot zCH_2Cl_2$ follows: $z = 0.58$, $VC_{24.58}H_{5.16}N_8Cl_{1.16}Br_4$, %C = 35.63 (35.82), %H = 0.99 (0.63), %N = 13.91 (13.60). For $V[TCNQMe_2]_2 \cdot zCH_2Cl_2$: $z = 0.86$, $VC_{28.86}H_{17.72}N_8Cl_{1.72}$, %C = 58.68 (58.91), %H = 3.57 (3.04), %N = 19.73 (19.04). For $V[TCNQEt_2]_2 \cdot zCH_2Cl_2$: $z = 0.02$, $VC_{32.02}H_{24.04}N_8Cl_{0.04}$, %C = 67.10 (67.09), %H = 4.54 (4.23), %N = 19.57 (19.55). For $V[TCNQ(i\text{-}Pr)_2]_2 \cdot zCH_2Cl_2$: $z = 0.60$, $VC_{36.6}H_{33.2}N_8Cl_{1.2}$, %C = 64.64 (64.78), %H = 4.86 (4.93), %N = 16.79 (16.51). For $V[TCNQ(OMe)_2]_2 \cdot zCH_2Cl_2$: $z = 0.50$, $VC_{28.5}H_{17}N_8ClO_4$, %C = 54.99 (55.05), %H = 2.80 (2.76), %N = 18.24 (18.02). For $V[TCNQ(OEt)_2]_2 \cdot zCH_2Cl_2$: $z = 0.70$, $VC_{32.0}H_{25.4}N_8Cl_{1.4}O_4$, %C = 56.42 (56.52), %H = 3.49 (3.68), %N = 16.40 (16.12). For $V[TCNQ(OPh)_2]_2 \cdot zCH_2Cl_2$: $z = 1.38$, $VC_{49.38}H_{26.76}N_8Cl_{2.76}O_4$, %C = 62.74 (62.77), %H = 2.65 (2.85), %N = 12.15 (11.86).

(6) Pokhodnya, K. I.; Epstein, A. J.; Miller, J. S. *Adv. Mater.* **2000**, *12*, 410.
(7) Pokhodnya, K. I.; Pejakovic, D.; Epstein, A. J.; Miller, J. S. *Phys. Rev. B* **2001**, *63*, 174408.
(8) Prigodin, V. N.; Raju, N. P.; Pokhodnya, K. I.; Miller, J. S.; Epstein, A. J. *Adv. Mater.* **2002**, *14*, 1230.
(9) Pokhodnya, K. I.; Petersen, N.; Miller, J. S. *Inorg. Chem.* **2002**, *41*, 1996.
(10) (a) Melby, L. R.; Harder, R. J.; Hertler, W. R.; Mahler, W.; Benson, R. E.; Mochel, W. E. *J. Am. Chem. Soc.* **1962**, *84*, 3374. (b) Kaim, W.; Moscherosch, M. *Coord. Chem. Rev.* **1994**, *129*, 157. (c) Zhao, H.; Heintz, R. A.; Ouyang, X.; Dunbar, K. R. *Chem. Mater.* **1999**, *11*, 736. (d) Long, G.; Willett, R. D. *Inorg. Chim. Acta* **2001**, *313*, 1−14. (e) Siedle, A. R.; Candela, G. A.; Finnegan, T. F. *Inorg. Chim. Acta* **1979**, *35*, 125. (f) Clérac, R.; O'Kane, S.; Cowen, J.; Ouyang, X.; Heintz, R.; Zhao, H.; Bazile, M. J.; Dunbar, K. R. *Chem. Mater.* **2003**, *15*, 1840−1850. (g) Heintz, R.; Zhao, H.; Ouyang, X.; Grandinetti, G.; Cowan, J.; Dunbar, K. R. *Inorg. Chem.* **1999**, *38*, 144−156.
(11) Pangborn, A. B.; Giardello, M. A.; Grubbs, R. H.; Rosen, R. K.; Timmers, F. J. *Organometallics* **1996**, *15*, 1518.
(12) Liu, X.; Ellis, J. E.; Selby, T. D.; Ghalsasi, P.; Miller, J. S. *Inorg. Synth.* **2004**, *34*, 68.
(13) Wheland, R. C.; Martin, E. L. *J. Org. Chem.* **1975**, *40*, 3101.
(14) Anderson, S. J.; Wells, F. J.; Wilkinson G. *Polyhedron* **1988**, *7*, 2615.
(15) Miller, J. S.; Kravitz, S. H.; Kirschner, S.; Ostrowski, P.; Nigrey, P. J. *J. Chem. Educ.* **1977**, *55*, 181; *Quant. Chem. Prog. Exch.* **1977**, *10*, 341.

$V[TCNQ]_x[TCNQ(OEt)_2]_{2-x}\cdot zCH_2Cl_2$. In a typical preparation, 1 equiv of $V(CO)_6$ and 2 equiv total of TCNQ and $TCNQ(OEt)_2$ were each dissolved in a minimum amount of CH_2Cl_2; the $V(CO)_6$ solution was then added dropwise to the stirred, filtered solution of TCNQ and $TCNQ(OEt)_2$. The solution quickly turned dark with the evolution of CO and was allowed to react 10 min at room temperature and 10 min at −20 °C without stirring, but with venting. The dark, amorphous product was filtered and dried (yield ∼80%). The observed elemental analysis (calcd) for $V[TCNQ]_x[TCNQ(OEt)_2]_{2-x}\cdot zCH_2Cl_2$ follows: $x = 1.8$, $z = 1.49$, $VC_{26.29}H_{12.98}N_8Cl_{2.98}O_{0.4}$, %C = 52.01 (52.29), %H = 1.92 (2.17), %N = 18.85 (18.56); $x = 1.6$, $z = 1.08$, $VC_{26.68}H_{13.36}N_8Cl_{2.16}O_{0.8}$, %C = 54.43 (54.66), %H = 2.38 (2.30), %N = 19.51 (19.11); $x = 1.0$, $z = 0.81$, $VC_{28.81}H_{17.62}N_8Cl_{1.62}O_2$, %C = 55.85 (56.16), %H = 2.83 (2.88), %N = 18.67 (18.18); $x = 0.6$, $z = 0.81$, $VC_{30.41}H_{20.82}N_8Cl_{1.62}O_{2.8}$, %C = 56.01 (56.07), %H = 2.98 (3.22), %N = 17.40 (17.20); $x = 0.4$, $z = 1.07$, $VC_{31.47}H_{22.94}N_8Cl_{2.14}O_{3.2}$, %C = 54.58 (54.69), %H = 3.53 (3.35), %N = 16.46 (16.21).

Powder samples for magnetic measurements were loaded in airtight Delrin holders and packed with oven-dried quartz wool to prevent movement of the sample in the holder. The dc magnetization temperature dependence was obtained by cooling in zero field, and then, data was collected on warming in 5 or 1000 Oe external magnetic field using a Quantum Design MPMS-5XL 5 T SQUID magnetometer equipped with a reciprocating sample measurement system, low field option, and continuous low-temperature control with enhanced thermometry features. The T_c's were obtained from an extrapolation of the low-field $M(T)$ to the temperature at which $M(T) \rightarrow 0$ as used in determining T_c of $V[TCNE]_y\cdot zCH_2Cl_2$.[4a,7] The ac magnetic susceptibility was measured in 1 or 3 Oe ac field (zero dc applied field), at 33, 100, and 1000 Hz. Phase sensitive lock-in detection allowed both the in-phase (χ') and out-of-phase (χ'') linear susceptibilities to be extracted.

Thermogravimetric analysis (TGA) was performed on a TA Instruments TGA 2050 analyzer. Infrared spectra were obtained using Bruker Tensor 37 FTIR spectrometer (±1 cm^{-1}). Elemental analyses were performed by Complete Analysis Laboratories Inc. of Parsippany, NJ.

Ab initio UB3LYP/6-31++g(d,p) calculations were executed using the nonlocal B3LYP exchange and correlation DFT[16] with the 6-31++g(d,p) basis set.[17] All calculations were done using the Gaussian-03 suite of programs.[18] The optimized structure of each $[TCNQ]^{\bullet-}$ derivative was based on the structure of $[TCNQ]^{\bullet-}$ [19] where the hydrogen atoms in the 2 and 5 positions were replaced by R (R= Br, Me, Et, *i*-Pr, OMe, OPh, and OEt). Each radical anion, including $[TCNQ]^{\bullet-}$, was then optimized completely using Gaussian's geometry optimization procedures at the UB3LYP/31++g(d,p) level. Mulliken and natural bond order (NBO) charge and spin distributions were calculated.[20] NBO spin densities were determined using the code word pop = NBO, where separate α and β electron populations were found for each unique atom within the $[TCNQR_2]^{\bullet-}$ anion. The α and β populations then allowed the spin density to be calculated as the difference between the α and the β electron populations.[21]

(16) The B3LYP is a combination of the nonlocal three parameters exchange functional [Becke, A. D. *J. Chem. Phys.* **1993**, *98*, 5648] and nonlocal LYP correlation functional [Lee, C.; Yang, W.; Parr, R. G. *Phys. Rev. B* **1998**, *37*, 785].

(17) (a) Ditchfield, R.; Hehre, W. J.; Pople, J. A. *J. Chem. Phys.* **1971**, *54*, 724. (b) Clark, T.; Chandrasekhar, J.; Spitznagel, G. W.; Schleyer, R. v. R. *J. Comput. Chem.* **1983**, *4*, 294.

Results and Discussion

Magnetically ordered $V[TCNE]_y$ can by synthesized by the reaction of $V^0(CO)_6$[5] or $V^0(C_6H_6)_2$[4] with TCNE. Mechanistic studies with $V^0(C_6H_6)_2$ reveal that 2 equiv of TCNE are reduced, forming $[TCNE]^{\bullet-}$ and V(II).[22] In contrast, none of the acceptors discussed herein have an oxidation potential sufficient to oxidize $V(CO)_6$ [$E^{-/0} = +0.88$ V vs SCE (CH_2Cl_2)[23]]. Nonetheless, immediate reactions occur between $V(CO)_6$ and **2a**−**g** to form dark, amorphous products (eq 4). Putatively, this reaction proceeds via an associative reaction, leading to disproportionation of $V(CO)_6$, as occurs for $V(CO)_6$ and MeCN.[24] The products decompose in the ambient laboratory atmosphere and must be stored under N_2 at −20 °C.

$$V(CO)_6 + 2TCNQR_2 \rightarrow V[TCNQR_2]_2\cdot zCH_2Cl_2 + 6CO \quad (4)$$

Hence, unlike the reaction of $V(C_6H_6)_2$ and TCNE, the reaction of $V(CO)_6$ and the disubstituted TCNQs (and TCNE) must initially proceed by ligand substitution involving nucleophilic attack by an acceptor. This mechanism would lead to a seven-coordinate vanadium complex with reduced oxidation potential, which would immediately undergo a CO loss. The reaction is not, therefore, initiated by electron transfer as occurs in the formation of $V[TCNE]_y$ from $V(C_6H_6)_2$.

The $\nu_{C\equiv N}$ IR absorptions of $V[TCNQ]_2\cdot zCH_2Cl_2$ occur at 2190 (s), 2088 (s), and 2024 (sh) cm^{-1} (Figure 1; Table 1). These absorptions are lower in energy than that of $TCNQ^0$ at 2222 (s) cm^{-1} and indicate that the product has reduced TCNQ.[10f] The number and broad nature of the $\nu_{C\equiv N}$ stretches suggest that there are multiple C≡N environments in the material. This is observed for $V[TCNE]_y\cdot zCH_2Cl_2$ with a broad absorption at 2090 cm^{-1} and three relatively narrow

(18) Frisch, M. J.; Trucks, G. W.; Schlegel, H. B.; Scuseria, G. E.; Robb, M. A.; Cheeseman, J. R.; Montgomery, J. A., Jr.; Vreven, T.; Kudin, K. N.; Burant, J. C.; Millam, J. M.; Iyengar, S. S.; Tomasi, J.; Barone, V.; Mennucci, B.; Cossi, M.; Scalmani, G.; Rega, N.; Petersson, G. A.; Nakatsuji, H.; Hada, M.; Ehara, M.; Toyota, K.; Fukuda, R.; Hasegawa, J.; Ishida, M.; Nakajima, T.; Honda, Y.; Kitao, O.; Nakai, H.; Klene, M.; Li, X.; Knox, J. E.; Hratchian, H. P.; Cross, J. B.; Adamo, C.; Jaramillo, J.; Gomperts, R.; Stratmann, R. E.; Yazyev, O.; Austin, A. J.; Cammi, R.; Pomelli, C.; Ochterski, J. W.; Ayala, P. Y.; Morokuma, K.; Voth, G. A.; Salvador, P.; Dannenberg, J. J.; Zakrzewski, V. G.; Dapprich, S.; Daniels, A. D.; Strain, M. C.; Farkas, O.; Malick, D. K.; Rabuck, A. D.; Raghavachari, K.; Foresman, J. B.; Ortiz, J. V.; Cui, Q.; Baboul, A. G.; Clifford, S.; Cioslowski, J.; Stefanov, B. B.; Liu, G.; Liashenko, A.; Piskorz, P.; Komaromi, I.; Martin, R. L.; Fox, D. J.; Keith, T.; Al-Laham, M. A.; Peng, C. Y.; Nanayakkara, A.; Challacombe, M.; Gill, P. M. W.; Johnson, B.; Chen, W.; Wong, M. W.; Gonzalez, C.; Pople, J. A. *Gaussian 03*, revision B.02; Gaussian, Inc.: Pittsburgh, PA, 2003

(19) Miller, J. S.; Zhang, J. H.; Reiff, W. M.; Dixon, D. A.; Preston, L. D.; Reis, A. H.; Gebert, E.; Extine, M.; Troup, J.; Epstein, A. J.; Ward, M. D. *J. Phys. Chem.* **1987**, *91*, 4356.

(20) Glendening, E. D.; Reed, A. E.; Carpenter, A. E.; Weinhold, F. NBO Version 3.1.

(21) Szabo, A.; Ostlund, N. S. *Modern Quantum Chemistry: Introduction to Advanced Electronic Structure Theory*; Macmillan Publishing Co., Inc.: New York, 1982.

(22) Gordon, D. C.; Deakin, L.; Arif, A. M.; Miller, J. S. *J. Am. Chem. Soc.* **2000**, *122*, 290.

(23) Bond, A. M.; Cotton, F. A. *Inorg. Chem.* **1976**, *15*, 2036.

(24) (a) Richmond, T. G.; Shi, Q.-Z.; Trogler, W. C.; Basolo, F. *J. Am. Chem. Soc.* **1984**, *106*, 76. (b) Shi, Q.-Z.; Richmond, T. G.; Trogler, W. C.; Basolo, F. *J. Am. Chem. Soc.* **1984**, *106*, 71.

Table 1. Summary of the ν_{CN} IR and Magnetic Properties for V[TCNQR$_2$]$_2$·zCH$_2$Cl$_2$

TCNQ	z[a]	θ', K	μ_{eff}, μ_B (300 K)	T_c,[b] K	T_b,[c] K	M_s,[d] emu·Oe/mol	M_r,[e] emu·Oe/mol	H_{cr},[e] Oe	φ	$\nu_{C\equiv N}$, cm^{-1}
TCNQ from [TCNQ]$^{\bullet-}$										2197s, 2113s
TCNQ	0.84	58	3.57	52	35	8075	2500	75	0.01	2190s, 2088s, 2024 sh
2,5-TCNQBr$_2$	0.58									2197, 2102 br
2,5-TCNQMe$_2$	0.86	15	3.57	7.5	4	7050	120	40	0.04	2189s, 2080s, 2010 sh
2,5-TCNQEt$_2$	0.02	52	3.40	17	12	6825	940	115	0.00	2190s, 2074s, 2010 sh
2,5-TCNQ(*i*-Pr)$_2$	0.60	15	3.55	9	7	6775	60	35	0.03	2188s, 2075s, 2010 sh
2,5-TCNQ(OMe)$_2$	0.50	85	3.71	61	44	6675	1700	20	0.00	2191s, 2095s, 2030 sh
2,5-TCNQ(OEt)$_2$	0.70	115	4.24	106	85	8850	2000	20		2190s, 2088s, 2030 sh
2,5-TCNQ(OPh)$_2$	1.38	30	4.26	20	15	6745	500	25	0.06	2190s, 2091s, 2020 sh

[a] Calcd from the elemental analysis data. [b] Obtained from an extrapolation of the low-field $M(T)$ to the temperature at which $M(T) \rightarrow 0$. [c] FC/ZFC bifurcation temperature. [d] M at 5 T and 2 K, as none of samples reach saturation. [e] 2 K.

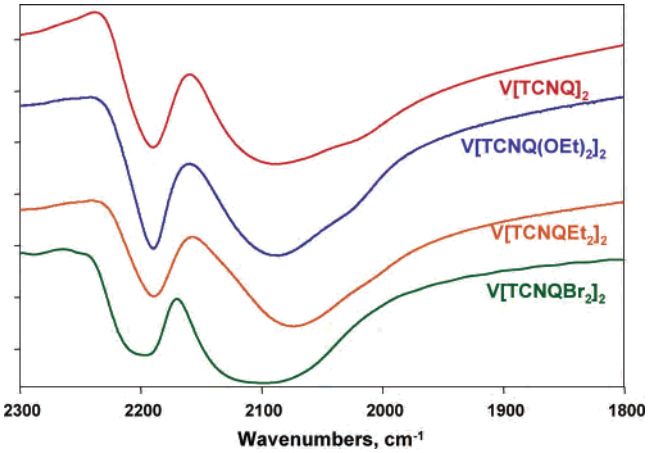

Figure 1. $\nu_{C\equiv N}$ region of the IR spectra of V[TCNQR$_2$]$_2$·zCH$_2$Cl$_2$ for R = H, OEt, Et, and Br.

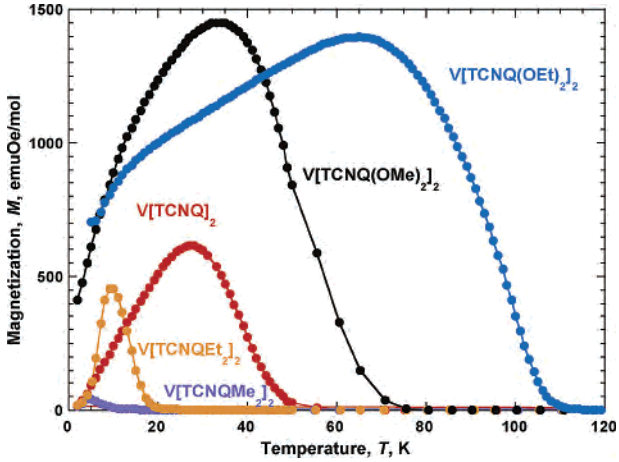

Figure 2. $M(T)$ 5 Oe for V[TCNQ]$_2$·0.84CH$_2$Cl$_2$ (red), V[TCNQMe$_2$]$_2$·0.86CH$_2$Cl$_2$ (purple), V[TCNQEt$_2$]$_2$·0.02CH$_2$Cl$_2$ (orange), V[TCNQ(OMe)$_2$]$_2$·0.50CH$_2$Cl$_2$ (black), and V[TCNQ(OEt)$_2$]$_2$·0.70CH$_2$Cl$_2$ (blue).

features at 2214, 2191, and 2152 cm^{-1}.[5,7] The highest energy $\nu_{C\equiv N}$ absorption remains the same for V[TCNQR$_2$]$_2$·zCH$_2$Cl$_2$ except for R = Br, which shows a shift from 2190 to 2197 cm^{-1}. The middle band also shifts to higher energy for R = Br, moving from 2088 to 2102 cm^{-1}, and appears at lower energy for the alkyl-substituted materials. It should be noted that the shoulder at lower energy seems to correlate qualitatively with the magnetic ordering of the materials, as those without it (V[TCNQ]$_2$ from [V(NCMe)$_6$](BPh$_4$)$_2$ and V[TCNQBr$_2$]$_2$) do not order magnetically. The position of the lower energy peak is slightly shifted to higher energy for the alkoxy-substituted TCNQs and to lower energy for the alkyl-substituted TCNQs. Some aliphatic ν_{C-H} stretches occur below 3000 cm^{-1}, indicative of the presence of CH$_2$Cl$_2$ solvent. The presence of solvent is also supported by the TGA data and elemental analysis results.

Magnetic Studies. The 2 to 300 K magnetization, $M(T)$, was determined at 1000 Oe for each material (Figure 2). The data for each material can be fit to the Curie−Weiss expression with θ' values dependent on the identity of R and indicative of effective ferrimagnetic behavior (Table 1). The $\chi^{-1}(T)$ data is generally linear in the region immediately above T_c, but d[$\chi^{-1}(T)$]/dT decreases above this region, indicative of longer range antiferromagnetic coupling. Values of μ_{eff} [$\equiv(8\chi T)^{1/2}$] are in the range 3.40 μ_B (R = Et) to 4.26 μ_B [R = OEt, OPh)] and are lower than the theoretical value of 4.58 μ_B. The zero-field cooled (ZFC) and field cooled (FC) $M(T)$ data were determined at 5 Oe and showed bifurcation points between 4 and 85 K. Ordering temperatures, T_c, range from 7.5 (R = Me) to 106 K (R = OEt) and are obtained from an extrapolation of the low-field $M(T)$ values to the temperatures at which $M(T) \rightarrow 0$ for each material. This indicates that magnetically ordered materials of V[TCNQR$_2$]$_2$·zCH$_2$Cl$_2$ composition are obtained for R = H, Me, Et, *i*-Pr, OMe, OEt, and OPh. Due to the extreme air sensitivity of the materials discussed herein, this method of finding the onset temperature of magnetization is assumed to be correct within ±3 K.

Field-dependent isothermal magnetization, $M(H)$, was determined on each material at 2 K (Figure 3). In general, each curve shows a sharp increase below ~100 Oe followed by a gentle upward slope to 5 T, at which point the magnetization reaches near-saturation, i.e., 6675−8850 emu·Oe/mol. These values are higher than the expected value of 5585 emu·Oe/mol for $S = {}^3/_2$ V^{II} antiferromagnetically coupled to two $S = {}^1/_2$ [TCNQR$_2$]$^{\bullet-}$ but far too low to indicate ferromagnetic coupling (i.e., 16,750 emu·Oe/mol); therefore, the materials are ferrimagnets. The origin of these higher-than-expected values is unknown. However, due to the disorder and amorphous nature of these materials, it is attributed to a lack of totally antiparallel alignment of the $S = {}^3/_2$ V^{II} spins with the two $S = {}^1/_2$ [TCNQR$_2$]$^{\bullet-}$ spins, resulting in a value that indicates that the uncompensated spin exceeds $^1/_2$. This would be sample-dependent, and variations in M at 5 T were observed between samples of the same nominal composition. The magnetization slopes are steeper at high fields for those materials with lower T_c values,

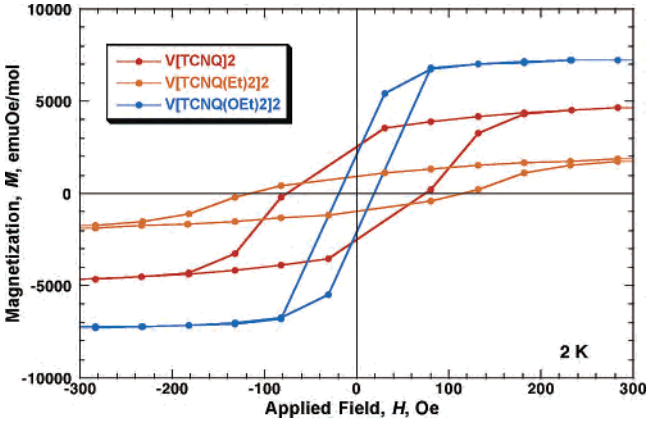

Figure 3. 2 K $M(H)$ showing hysteretic behavior for $V[TCNQ]_2 \cdot 0.84CH_2Cl_2$ (red), $V[TCNQEt_2]_2 \cdot 0.02CH_2Cl_2$ (orange), and $V[TCNQ(OEt)_2]_2 \cdot 0.70CH_2Cl_2$ (blue).

namely, R = Me, Et, *i*-Pr, and OPh. The systems show coercive fields (H_{cr}) between 20 Oe (R = OMe) and 115 Oe (R = Et) at 2 K, suggesting that they are moderately soft ferrimagnets. Substitution of an R group decreases H_{cr} relative to R = H except in the case of R = Et, which increases H_{cr} to 115 Oe. The remanant magnetization (M_r) of $V[TCNQ]_x \cdot zCH_2Cl_2$ is 2500 emu·Oe/mol at 2 K; however, each of the materials from disubstituted TCNQs exhibits a lower M_r than 2500 emu·Oe/mol at 2 K, particularly those with reduced T_c's (R = Me, Et, *i*-Pr, OPh).

The temperature dependencies of the in-phase, $\chi'(T)$, and out-of-phase, $\chi''(T)$, components of ac susceptibility at 33, 100, and 1000 Hz were measured. Each material exhibited a single peak in both χ' and χ'' except R = OEt, which had very broad peaks in both χ' and χ'' that seemed to suggest multiple phases. A small frequency dependence was observed for R = H, Me, *i*-Pr, OPh. Substantial $\chi''(T)$ signals support the proposal that the materials are ferrimagnets.

MO Calculations. The addition of highly electron-donating alkoxy groups raised the ordering temperature, whereas the addition of less electron-donating alkyl groups[25] reduced the ordering temperature and the addition of electron-withdrawing bromo groups resulted in a product that was not magnetically ordered. The origin of this trend is unknown, but it may arise from changes in either the spin or charge distribution as the R group was varied. Increasing the spin density at the nitrile nitrogens correlated with an increase in the spin coupling. Likewise, the more electron density that is donated into the nitrile nitrogens from the R groups, the more strongly they can bond to vanadium. Either of these stronger interactions may then result in a larger magnetic coupling energy, J, which can lead to higher magnetic ordering temperatures. In order to test this hypothesis, Mulliken and NBO spin and charge calculations were performed using the B3LYP functional within DFT and the UB3LYP/6-31++g(d,p) basis set. The spin density was calculated to be 0.29, −0.06, and 0.15 for the sp^2-C, sp-C, and N, respectively, for $[TCNE]^{\bullet -}$, in excellent agreement with 0.29, −0.04, and 0.16 previously reported.[26]

(25) Hansch, C.; Leo, A.; Taft, R. W. *Chem. Rev.* **1991**, *91*, 165.

Charge Distributions. The Mulliken charge distribution (Table S1) differs significantly from NBO charge distribution (Table S2). The charge distribution for C5 and C6 varies from 0.01 for R = OPh to 0.32 for R = Et for the Mulliken charge distribution, but only between 0.01 for R = OMe and OEt and 0.09 for R = *i*-Pr.[27a] The same trend is seen for N1 and N2. No significant correlation between T_c and the charge distribution is observed except for a mild trend with C3 and T_c, as the charge on C3 becomes more negative with increasing T_c. No trend was observed from the NBO charge distributions.

Spin Density. Mulliken spin densities showed no correlation between the spin densities of the atoms of $[TCNQR_2]^{\bullet -}$ and T_c. The atomic spin densities change insignificantly with R (Table S3). Overall trends, however, show that C4 has the greatest spin density (0.33−0.28), followed by N1 and N2 (0.14−0.11). C5 and C6 have the most negative spin density (−0.11 to −0.07). The same trends were seen for the NBO spin densities, but the magnitudes of the values are reduced (Tables S4, S5, and S6). From NBO calculations, the C4 spin density ranges from 0.25 to 0.22, while N1 and N2 range between 0.13 and 0.01, and C5 and C6 range from −0.05 to −0.04.[27b] For comparison, the spin density of $[TCNE]^{\bullet -}$ was determined using the same method. It was found that the spin density determined by NBO was in better agreement with past spin density results calculated by DFT than the Mulliken spin density (Table S7).[26] Spin contamination was evident for R= *i*-Pr, Et, OPh (Table S8), as the β populations for these radical anions are not zero; however, the degree of contamination is insignificant.

Experimental versus Calculated Spin Densities. The observed spin distribution for $[TCNE]^{\bullet -}$ obtained from EPR studies[28] is in better agreement with the NBO-calculated spin density (Table S9). The difference between the NBO and EPR spin distributions is also noted for $[TCNE]^{\bullet -}$, where it was shown that single crystal polarized neutron diffraction data was more accurate in determining the spin density, Table S10. Thus, the spin density determined by NBO calculations is preferred for predicting the spin density on each atom.[26]

According to the results obtained from Mulliken and NBO calculations, neither the change in charge nor spin distributions for $[TCNQR_2]^{\bullet -}$, as R is changed from electron donating to electron withdrawing groups, can explain the wide range of critical temperatures.

$V[TCNQ]_x[TCNQ(OEt)_2]_{2-x} \bullet zCH_2Cl_2$ Solid Solutions. Solid solutions of $V[TCNQ]_x[TCNQ(OEt)_2]_{2-x} \cdot zCH_2Cl_2$ composition were prepared via eq 5. The syntheses of the solid

(26) Zheludev, A.; Grand, A.; Ressouche, E.; Schweizer, J.; Morin, B.; Epstein, A. J.; Dixon, D. A.; Miller, J. S. *J. Am. Chem. Soc.* **1994**, *116*, 7243. Zheludev, A.; Grand, A.; Ressouche, E.; Schweizer, J.; Morin, B. G.; Epstein, A. J.; Dixon, D. A.; Miller, J. S. *Angew. Chem.* **1994**, *33*, 1397.

(27) For $[TCNQR_2]^{\bullet -}$ (R = Me, *i*-Pr, Et OPh), the symmetry of the geometry-optimized structure is not preserved for C1, C2, C3, and C4; hence, the reported values are an average over C1′, C2′, C3′, and C4′, respectively. (a) Fixing the symmetry did not correct the problem. (b) The maximum difference between the α and β electron populations was only 0.004 for C1 of R = OPh.

(28) Kaplan, M. L.; Haddon, R. C.; Bramwell, F. B.; Wudl, F.; Marshall, J. H.; Cowan, D. O.; Gronowitz, S. *J. Phys. Chem.* **1980**, *84*, 427−431.

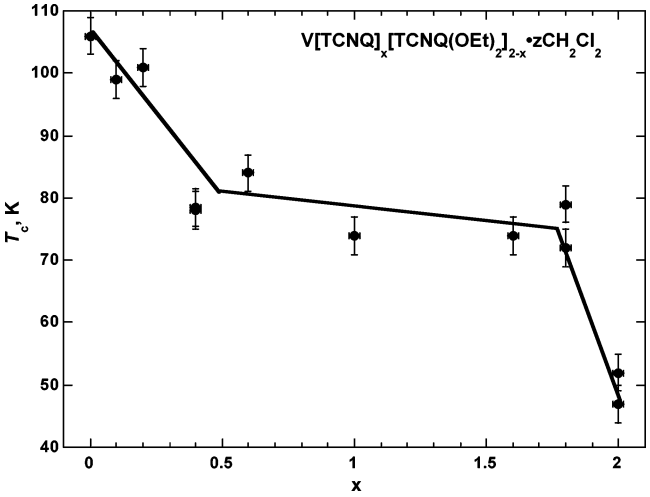

Figure 4. T_c as a function of x for V[TCNQ]$_x$[TCNQ(OEt)$_2$]$_{2-x}$•zCH$_2$Cl$_2$.

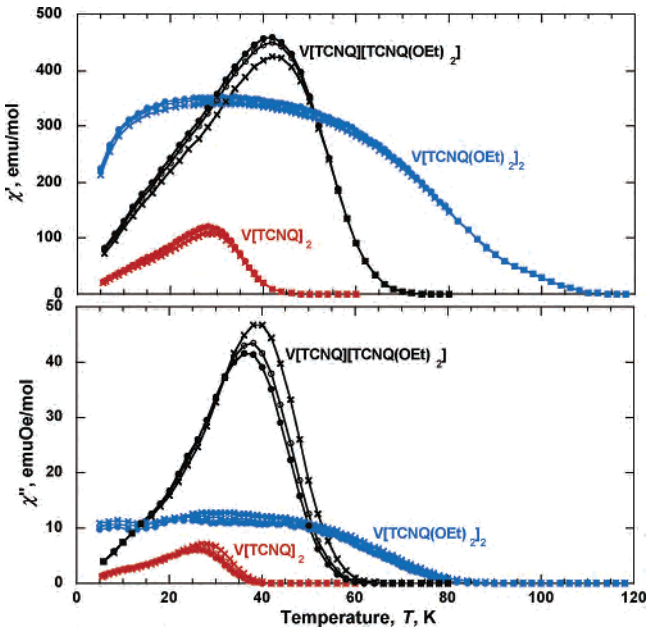

Figure 5. Real, $\chi'(T)$, and imaginary, $\chi''(T)$, ac susceptibilities for V[TCNQ]$_2$•0.84CH$_2$Cl$_2$ (red), V[TCNQ(OEt)$_2$]$_2$•0.70CH$_2$Cl$_2$ (blue), and V[TCNQ][TCNQ(OEt)$_2$]•0.81CH$_2$Cl$_2$ (black) at 33 (●), 100 (○), and 1000 (×) Hz.

solutions were difficult to control due to the different solubilities of the acceptors, the differing reaction rates of the acceptors with $V(CO)_6$, and the extreme air sensitivity of the products. The IR spectra showed $\nu_{C\equiv N}$ absorptions at 2192 and 2088 cm^{-1} with slight shoulders at lower energy, but no strong correlation to x in the C≡N region. However, a general trend was observed in the 1600−1500 cm^{-1} region. A strong absorbance at ∼1575 cm^{-1} for $x = 2$ gradually shifted to 1585 cm^{-1} and decreased in intensity as x was decreased, consistent with formation of a solid solution and not of a physical mixture. The magnetic properties of V[TCNQ]$_x$[TCNQ(OEt)$_2$]$_{2-x}$•zCH$_2$Cl$_2$ ($x = 0$, 0.1, 0.2, 0.4, 0.6, 1.0, 1.4, 1.8, and 2.0) were examined with the expectation that T_c would vary in a linear manner as a function of x. T_c increases from ∼50 to ∼75 K as a small amount of TCNQ(OEt)$_2$ is added ($x = 1.8$), and then remains relatively steady from 78 ± 6 K for $0.4 \le x \le 1.8$ (Figure 4). This flat region is followed by a rapid increase in T_c to ∼105 K for $0 \le x \le 0.2$. Although the T_c values correspond to the x value (albeit not in a linear manner), the magnitude of both the $\chi'(T)$ and $\chi''(T)$ ac peaks are greater for $x = 1$ than for $x = 0$, 2 (Figure 5). For $x = 1$, $\varphi = 0.032$, indicating that there is indeed a larger degree of disorder in the mixed-ligand system than there is for R = H. The reason for the enhanced peak magnitudes is unknown but is being studied further. Hence, the observed data does not fit the expected trend, and the relationship between T_c and x appeared to be more of a step function than a first-order dependence. The genesis of this unexpected trend is unknown and under further study.

$$V(CO)_6 + x\text{TCNQ} + (2-x)\text{TCNQ(OEt)}_2 \rightarrow \text{V[TCNQ]}_x\text{[TCNQ(OEt)}_2\text{]}_{2-x} + 6\text{CO} \quad (5)$$

Conclusion

A new family of molecule-based magnets of general formula V[TCNQR$_2$]$_2$•zCH$_2$Cl$_2$ has been synthesized and characterized for R = H, Br, Me, Et, *i*-Pr, OMe, OEt, and OPh as well as a solid solution of V[TCNQ]$_x$[TCNQ(OEt)$_2$]$_{2-x}$•zCH$_2$Cl$_2$ composition. Magnetic ordering was observed for all materials except R = Br with T_c values between 7.5 K (R = Me) and 106 K (R = OEt). The substitution of electron donating alkoxy groups OMe and OEt increased T_c and decreased H_{cr} with respect to TCNQ, whereas the substitution of alkyl groups decreased T_c. Although it was hypothesized that this variation in T_c could be due in part to the variation of spin or charge density on the nitrile nitrogens due to the substitution groups, the results from MO spin and charge density calculations refute this hypothesis. The magnetic properties of V[TCNQ]$_x$[TCNQ(OEt)$_2$]$_{2-x}$•zCH$_2$Cl$_2$ deviated from the expected linear relationship with respect to x, exhibiting magnetic behavior more characteristic of a step function in a plot of $T_c(x)$.

On the basis of the structural similarity of TCNQ to TCNE, V[TCNQ]$_2$•zCH$_2$Cl$_2$ is proposed to possess a structure similar structure to V[TCNE]$_y$•zCH$_2$Cl$_2$. Hence, each TCNQ bonds on average to 3 V(II)'s, but locally it may bond to two or four with linear as well as some bent V−N≡C bonding (**3**). Each V(II) is proposed to be six-coordinate, bonding to as many as six different TCNQs. Consequently, a disordered, amorphous 3-D network structure forms as proposed for V[TCNE]$_y$•zCH$_2$Cl$_2$ except that the V···V separations are greater.

The enhanced T_c's of V[TCNQ(OMe)$_2$]$_2$•zCH$_2$Cl$_2$ (T_c = 61 K) and V[TCNQ(OEt)$_2$]$_2$•zCH$_2$Cl$_2$ (T_c = 106 K) with respect to V[TCNQMe$_2$]$_2$•zCH$_2$Cl$_2$ (T_c = 7.5 K) and V[TCNQEt$_2$]$_2$•zCH$_2$Cl$_2$ (T_c = 17 K) as well as V[TCNQ]$_2$•zCH$_2$Cl$_2$ (T_c = 52 K) suggest that the oxygen enhances the magnetic coupling. The contribution of resonance structures of [TCNQR$_2$]$^{\bullet-}$ results in nitrile nitrogens having some sp^2 character; therefore, they may participate in linear or bent bonding to vanadium. For example, the RuNC angle is 134.2° for [Ru(PPh$_3$)$_2$(TCNQ)]$_2$.[29] Linear V−N≡C bonding would, however, require the V−O separation (**3**, left side) to be too

large (ca. 4 Å) and directed incorrectly for significant interactions. In contrast, sp^2 hybridization of a nitrile C and N would enable formation of a seven-membered ring (**3**, right side), which could stabilize the structure and enhance the magnetic coupling, leading to an increased T_c. The larger OPh group would interfere and minimize this V—O interaction thereby decreasing T_c.

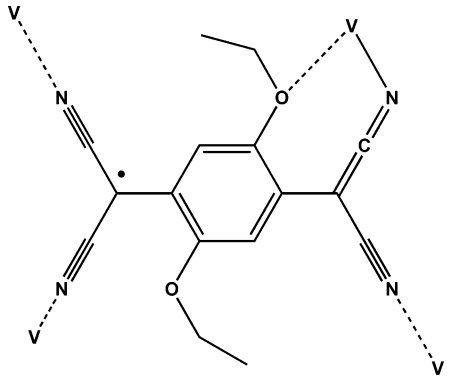

3

Acknowledgment. The authors gratefully acknowledge samples of **2e**,**f** kindly provided by Prof. G. Saito and H. Yamochi (Kyoto University) and helpful discussions with Profs. K. I. Pokhodnya, T. N. Truong, J. P. Simons, and J. J. Novoa, as well as the continued partial support by the Department of Energy Division of Materials Science (Grants DE-FG03-93ER45504, DE-FG02-01ER45931, DE-FG02-86ER45271, and DEFG0296ER12198), DARPA through ONR (Grant N00014-02-1-0593) and the Army Research Office (Grant DAAD19-01-1-0562).

Supporting Information Available: Calculated NBO and Mulliken charge and spin (α and β) distributions as well as total electron populations for $[TCNQR_2]^{\bullet-}$ and calculated spin distributions for $[TCNQ]^{\bullet-}$ and $[TCNE]^{\bullet-}$ for comparison with experimental values. This material is available free of charge via the Internet at http://pubs.acs.org.

IC049552Z

(29) Ballester, L.; Barral, M. C.; Gutiérrez, A.; Jiménez-Aparicio, R.; Martínez-Muyo, J. M.; Perpiñan, M. F.; Monge, M. A.; Ruíz-Valero, C. *J. Chem. Soc., Chem. Commun.* **1991**, 1396.